



Montmorillonite-based porous clay heterostructures (PCHs) intercalated with silica–titania pillars—synthesis and characterization

Lucjan Chmielarz^{a,*}, Barbara Gil^a, Piotr Kuśtrowski^a, Zofia Piwowarska^a, Barbara Dudek^a, Marek Michalik^b

^a Jagiellonian University, Faculty of Chemistry, Ingardena 3, 30-060 Kraków, Poland

^b Jagiellonian University, Institute of Geological Sciences, Oleandry 2a, 30-063 Kraków, Poland

ARTICLE INFO

Article history:

Received 18 November 2008

Received in revised form

2 February 2009

Accepted 10 February 2009

Available online 21 February 2009

Keywords:

Porous clay heterostructures (PCHs)

Montmorillonite

Silica–titania pillars

ABSTRACT

Porous clay heterostructures (PCHs) were synthesized using natural montmorillonite as a raw material. Apart from pure silica pillars also silica–titania pillars were intercalated into the interlayer space of the parent clay. The detailed studies of the calcination process of the as-prepared PCH samples as well as thermal stability of the pillared structure of these materials were performed. The pillared structure of PCHs intercalated with both silica and silica–titania clusters was found to be thermally stable up to temperatures exceeding 600 °C. It was found that titanium incorporated into the silica pillars was present mainly in the form of separated tetracoordinated cations. For the samples with the higher Ti loading also small contribution of titanium in the form of the polymeric oxide species was detected. Titanium incorporated into the PCH materials significantly increased their surface acidity forming mainly Brønsted acid sites.

© 2009 Elsevier Inc. All rights reserved.

1. Introduction

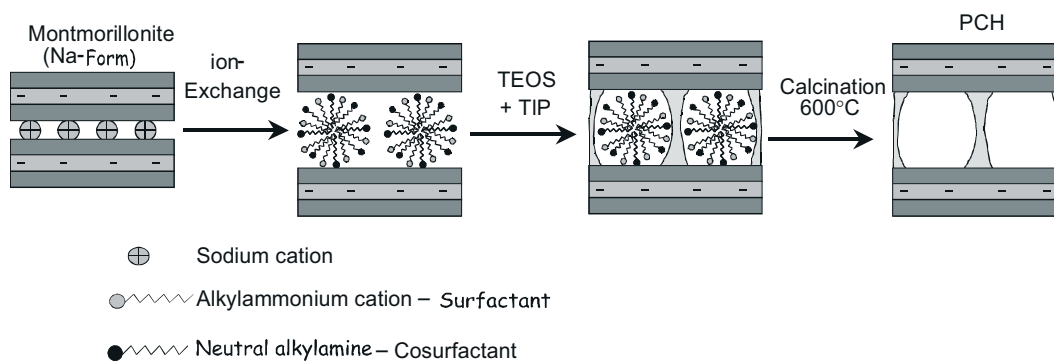
Clays, which belong to the phyllosilicate group, are very interesting materials for catalysis and adsorption. Acid-treated montmorillonites were successfully used as cracking catalysts [1]. On the other hand, cationic clay minerals are known to be excellent adsorbents, which could be used for elimination of various organic compounds from water [2]. Clays, which belong to the phyllosilicate group, can be relatively easily intercalated with metal oxide pillars. Deposition of such pillars into the interlayer space resulted in a significant increase of surface area and microporosity of the clay materials. A large number of metal oxide pillars such as Al₂O₃, TiO₂, and ZrO₂, has been successfully incorporated into different types of smectites [e.g. 3,4]. The pillared clays modified with the selected transition metals have been found to be active and selective catalysts of various reactions, including the DeNO_x process [e.g. 5,6] as well as were used for the elimination of various organic pollutants from waste water (e.g. phenol [7]). However, the structure of the pillared clays is not stable at higher temperatures [e.g. 8–10] and therefore applications of such materials are limited only to the low- and medium-temperature processes.

In 1995 Galarneau et al. [11] proposed a different way to obtain thermally stable porous materials from the cationic layered clays.

* Corresponding author. Fax: +48 126340515.

E-mail address: chmielar@chemia.uj.edu.pl (L. Chmielarz).

The synthesis of such materials consists of the following steps: (i) cationic templates and neutral amine co-templates are intercalated in the interlayer space of the host clay forming the micelle structures; (ii) the silica pillars are created by in-situ polymerization of a silica source around the micelle structures and (iii) the organic templates are removed from the material by a classical calcination, producing materials with a high surface area and combined micro and mesoporous structure. This new class of materials is called porous clay heterostructure (PCH). The synthesis procedure of montmorillonite based PCH is presented in Scheme 1. The negative charge of the clay layers is compensated by protons formed during the decomposition of the organic templates. Protons can migrate into unoccupied position in the clay layers (octahedral vacancies in dioctahedral clays or defects in trioctahedral clays) and in consequence reduce a cation exchange capacity (CEC) potential of PCHs. This effect can be limited by exchanging the protons for NH₄⁺ cations, which are too large to migrate into the clay layers [12]. The very important feature of the PCH materials is their surface acidity. Acid centers are located on surface of the clay layers and therefore, surface acidity is mainly related to the acidity of the parent clay used for the synthesis of PCHs. Various types of the cationic layered clays (fluorohectorite [11], montmorillonite [13], synthetic saponite [14], magadiite [15], vermiculite [16]) characterized by different surface acidity were used as precursors for the synthesis of the PCH materials. There is none or only a very small concentration of acid sites located on the silica interlayer pillars. The acidity of the PCH materials can be increased by an incorporation of the suitable



Scheme 1. Mechanism of the PCH synthesis.

cations (e.g. Ti, Al) into the silica walls. This method of the acid sites generation was developed and optimised for a large group of mesoporous silicas [e.g. 17–20]. On the other hand the number of papers related to the modifications of the surface acidity of PCHs is limited [21,22]. The paper presents synthesis and characterization of the montmorillonite-based PCH materials, intercalated with the silica–titania pillars. Much attention was paid to the thermal degradation of templates present in the pore system of as prepared PCHs as well as their thermal stability and surface acidity.

2. Experimental

2.1. Materials

Natural montmorillonite (CEC = 82 meq/100 g, $S_{\text{BET}} = 77 \text{ m}^2/\text{g}$, S&B Industrial Minerals GmbH) was used as a starting material for the preparation of a series of Ti-containing PCHs. Montmorillonite was not purified before its modification. In the first step parent montmorillonite was transformed into the sodium form (Na-Mont) by its treatment with a solution (1.0 M) of NaCl. Subsequently, the modified clay (6 g) was added to a solution (0.1 M; 100 ml) of surfactant (hexadecyltrimethylammonium chloride—HDTMA, Fluka) and stirred at 50 °C for 24 h. Then, the clay (HDTMA-Mont) was separated from the solution and washed with demineralised water till pH of 7 was reached. In the next step, the modified clay was divided into four parts. Each portion of montmorillonite modified with surfactant was added to melted hexadecylamine (HDA, Fluka), which played a role of co-surfactant. Subsequently, the mixture of tetraethylorthosilicate (TEOS, Fluka) and titanium isopropoxide (TIP, Fluka) was added into each suspension and was allowed to react for 4 h under continuous stirring. The following molar ratios of HDTMA/HDA/TEOS/TIP were applied: 1/20/150/0, 1/20/148.5/1.5, 1/20/142.5/7.5 and 1/20/135/15 for the production of the samples, which respectively are denoted as PCH, PCH-1.5Ti, PCH-7.5Ti and PCH-15Ti. After that the modified clays were separated from the solutions, washed with pure ethanol, dried at room temperature and finally calcined at temperatures 550, 600 or 800 °C for 6 h.

2.2. Methods

Thermogravimetric analysis of non-calcined PCHs was performed on Mettler Toledo TGA/SDTA 851^e connected on-line with quadrupole mass spectrometer (ThermoStar, Balzers). The measurements have been performed in the temperature range of 25–1000 °C with a heating ramp of 10 °C/min in a continuous flow

of synthetic air (80 ml/min). The following ions were monitored by QMS: $m/e = 2, 12, 14, 16, 17, 18, 28, 30, 32, 44, 45, 46, 58, 59$.

Chemical compositions of the sodium form of montmorillonite and PCH samples were determined by electron microprobe analysis performed on a JEOL JCA 733 superprobe microanalyzer (electron probe microanalysis—EPMA).

The X-ray diffraction patterns of the samples were obtained using a Philips X'Pert APD diffractometer using $\text{CuK}\alpha$ radiation ($\lambda = 0.154 \text{ nm}$). The 2θ range was varied from 1° to 85° with a step of 0.02°.

Textural parameters of the samples were determined by N_2 sorption at $-196 \text{ }^\circ\text{C}$ using an ASAP 2010 (Micromeritics) automated gas adsorption system. Prior to the analysis, the samples were outgassed under vacuum at 350 °C for 16 h. The specific surface areas S_{BET} were determined using the BET equation for the adsorption data in a relative pressure range p/p_0 from 0.05 to 0.20. Mesopore size distributions were determined using the BJH model.

The UV–vis–DR spectra of the samples were recorded using an Evolution 600 (Thermo) spectrophotometer. The measurements have been performed in the range of 200–900 nm with a resolution of 2 nm.

Surface acidity (concentration and strength of acid sites) of PCHs was studied by temperature programmed desorption of ammonia (NH_3 -TPD). The measurements were performed in a flow microreactor system equipped with QMS detector (VG Quartz). Prior to ammonia sorption, a sample was outgassed in a flow of pure helium at 600 °C for 1 h. Subsequently, the microreactor was cooled to 70 °C and the sample was saturated in a flow of gas mixture containing 1 vol% of NH_3 in helium for about 30 min. Then, the solid was purged in a helium flow until a constant baseline level was attained. Desorption was carried out with a linear heating rate (10 °C/min) in a flow of He (20 ml/min). Traces of H_2O and O_2 in pure helium (grade 5), used as the eluant gas, were removed by appropriate traps (Alltech). Calibration of QMS with commercial mixtures allowed recalculating the detector signal into the rate of NH_3 evolution.

The chemical nature of surface acid sites was studied by adsorption of pyridine, followed by IR spectroscopy. Transmission IR spectra (in absorbance mode) were recorded using wafers in the form of self-supporting pellets of the clay powder (ca. 10 mg/cm²). The pellet was placed in an IR cell designed to carry out spectroscopic measurements at different temperatures and equipped with CaF_2 windows. The cell was connected to a vacuum line allowing all thermal treatments and adsorption–desorption experiments to be carried out in situ. Prior to pyridine adsorption, the sample was outgassed at 480 °C under vacuum for 1 h. Then the cell was cooled to 170 °C and the solid material was allowed to react with pyridine for 10 min, subsequently weakly adsorbed

pyridine was evacuated for 20 min under vacuum. FTIR spectra were recorded on a Bruker Tensor 27 spectrometer for the samples evacuated at 170, 250, 350 or 450 °C. A 100 scans were taken with a resolution of 2 cm⁻¹.

3. Results and discussion

The synthesis of the PCH materials is performed by the template directed method [23]. In the final step of the synthesis, the organic templates have to be removed from the pore system of the material. Typically, calcination of the as-prepared samples is used for this purpose. The other method, however significantly less popular, is the extraction of the organic material from the pore system of the as-prepared samples with suitable solvents [24]. The mechanism of thermal degradation of organic surfactants from the pore system of the mesoporous silica materials is very complex and still not fully recognized [25–27]. Large surfactants and co-surfactants of the templating agents like halides of quaternary amines or neutral alkylamines, which are used for the synthesis of the PCH materials, are degraded into various products under thermal treatment.

3.1. Thermal degradation of organic templates

The process of template degradation was studied by thermogravimetric analysis combined with on line analysis of gaseous products by QMS detector. Various products of the template degradation could be expected. Ryczkowski et al. [25] suggested formation of the following products during the thermal treatment of the as-prepared MCM-41 sample in a flow of oxidizing gas mixture (5% O₂ in He). The CH₂=NH₂⁺ ions (m/e = 30) could be produced in the mass spectrometer as a result of a fragmentation of the alkylamine surfactant by the cleavage of the C–C bond in β position in relation to nitrogen. The m/e = 30 ions are also characteristic for NO, which could be expected as one of the products of alkylamines oxidation. In the cases of the process performed in air atmosphere, NO could be a result of the oxidation of the atmospheric N₂ at higher temperatures (thermal NO). The other products of the template oxidation are H₂O (m/e = 18) and CO₂ (m/e = 44). The m/e = 44 ion is also characteristic for N₂O, which could be another product of the alkylamine oxidation. Distinguishing between these two gases could be possible by additional analysis of the products of their fragmentation in the QMS detector—m/e = 28 (fragmentation of CO₂) and m/e = 14 (fragmentation of N₂O). The m/e = 28 ion is also characteristic for N₂, which could be expected as a product of surfactants oxidation. Ammonia (m/e = 17) is another possible product of the alkylamine degradation. The m/e = 17 ion is also a result of water fragmentation, therefore for the analysis of the NH₃ evolution by monitoring the m/e = 16 ion (the product of ammonia fragmentation) seems to be more suitable. However, this ion is also characteristic for the fragmentation of O₂ molecules. The m/e = 59 ion can be related to the evolution of trimethylamine –N(CH₃)₃– which is a result of alkylamine fragmentation by the reaction of Hoffman degradation. Additionally, in our studies we have included the analysis of the m/e = 46 ion characteristic for ethanol, which is a product of hydrolysis of TEOS. The analysis of the mechanism of the template degradation is a very difficult task, however it seems that such analysis performed with a combination of TGA and MS techniques can supply some important information related to this process.

Fig. 1 presents the results of TGA–MS analysis of the non calcined PCH sample. In the DTG curve four peaks can be found. The peak at about 76 °C could be related to the evaporation of small amount of ethanol (boiling point 78.4 °C), which is a product

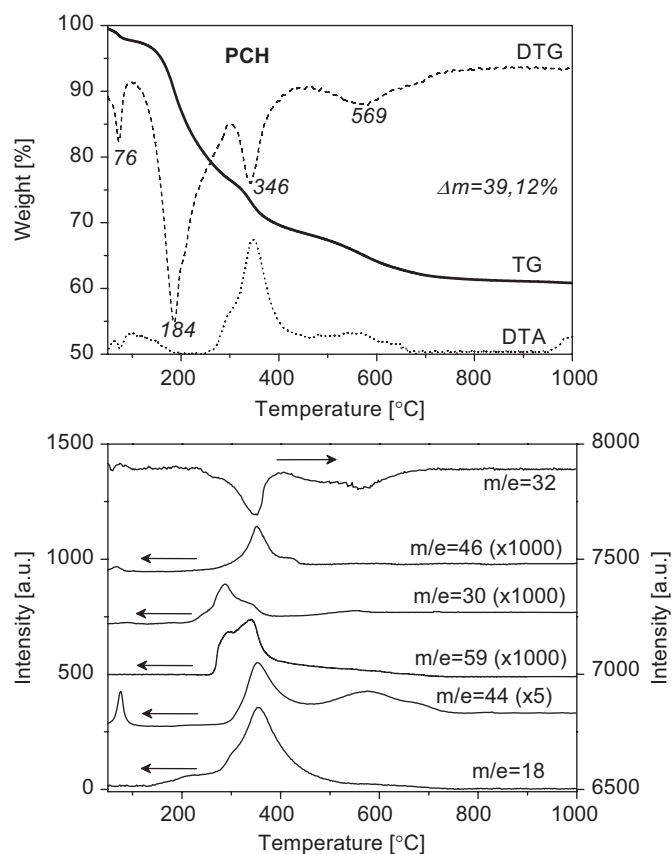


Fig. 1. Results of TG-DTA and evolved gas analysis of the as prepared PCH sample.

of TEOS hydrolysis and additionally was used for washing of PCHs after synthesis. On the other hand, maximum at 76 °C in a spectrum recorded for m/e = 44 line may suggest desorption of physically adsorbed CO₂. The next DTG peak is centered at 184 °C and is probably related to the desorption of products of the thermal degradation of surfactant and co-surfactant molecules. The process of aliphatic amines degradation is probably favored by the presence of the acid sites, located on the surface of the montmorillonite layers, which are known to be catalytically active in the process of hydrocarbons cracking [28]. The evolution of various compounds was detected at temperature above 140 °C. Evolution of water vapor (m/e = 18) started at 140 °C, however only small amounts of H₂O were detected below 280 °C. An increase in the intensity of the m/e = 30 ion signal was observed above 230 °C. As it was already mentioned, this ion can be related to the presence of CH₂=NH₂⁺ species formed by fragmentation (β position in relation to N atom) of HDA or formation of NO. Nitrogen oxide could be formed by the oxidation of alkylamines (so called “fuel NO”) or oxidation of atmospheric nitrogen (“thermal NO”). The later way of the nitrogen oxide formation is favored at high temperatures. The intensity of the m/e = 59 ions, which could be related to the evolution of trimethylamine N(CH₃)₃, increased from about 280 °C. Trimethylamine is probably formed by the reaction of Hoffman degradation of hexadecyltrimethylamine cations or, which is also possible, other aliphatic amines formed by the surfactants fragmentation. It should be mentioned that the evolution of trimethylamine at temperatures lower by about 120 °C was reported for MCM-41 [25]. This difference is probably related to chemisorption of the basic N(CH₃)₃ molecules on acidic sites present in the PCH materials. Pure silica MCM-41 materials do not contain or contain only a very small concentration of acid sites and therefore, the

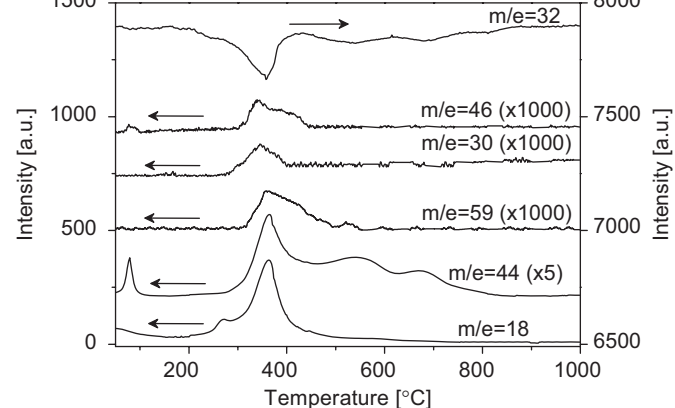
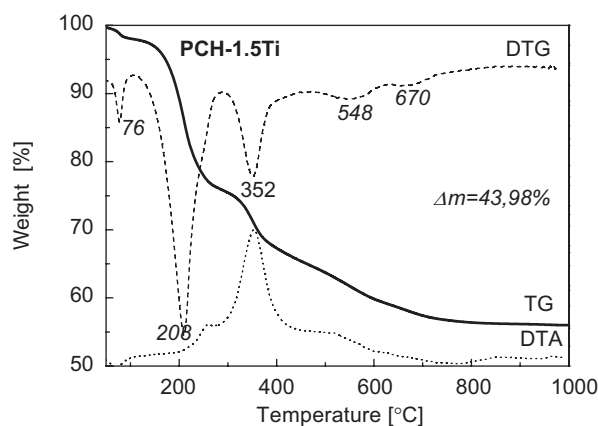


Fig. 2. Results of TG-DTA and evolved gas analysis of the as prepared PCH-1.5Ti sample.

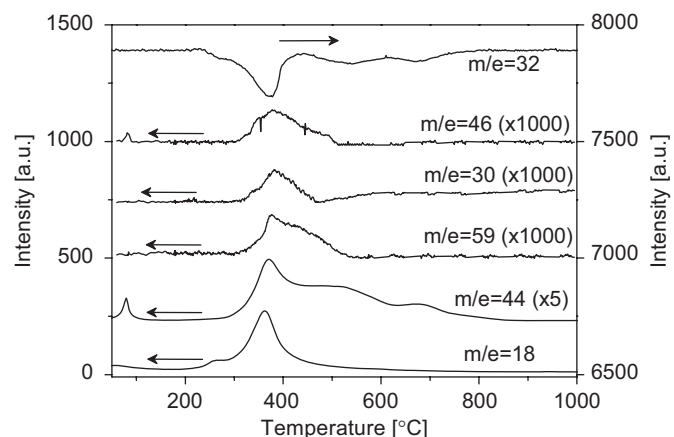
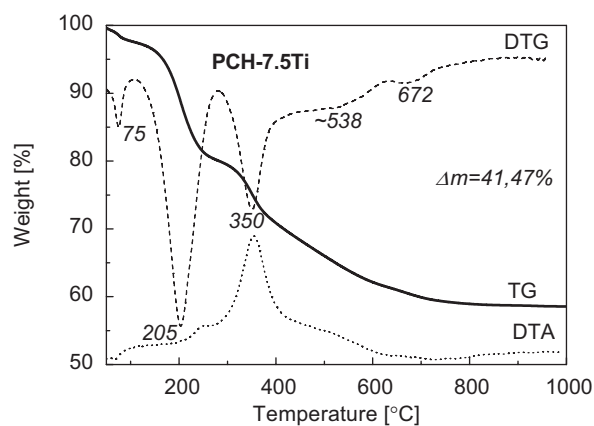
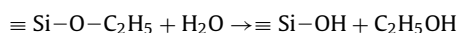


Fig. 3. Results of TG-DTA and evolved gas analysis of the as prepared PCH-7.5Ti sample.

interaction of trimethylamine molecules with the ordered silica surface has to be strongly limited. At higher temperatures, intensive oxidation of the organic matter deposited in the pore system of the PCH sample was detected. This process is accompanied by the weight loss (DTG curve, peak at 346 °C), exothermal heat effect (DTA curve), consumption of oxygen ($m/e = 32$) and formation of H_2O ($m/e = 18$) and CO_2 ($m/e = 44$). Additionally, the formation of the $m/e = 46$ ions in the temperature range of 300–450 °C was detected (Fig. 1). This effect is probably related to the evolution of ethanol molecules, which were formed by the hydrolysis of ethoxy species (residue species, which were not completely hydrolyzed during the intercalation of SiO_2 pillars). These reactions can be presented in the form of the following equation:



Alkoxy species are transformed into silanol groups and ethanol. Such hydrolysis processes did not occur at lower temperatures due to deficiency of water. Broad peak centered at temperature 569 °C can be found in the DTG curve. Evolution of CO_2 and intensive consumption of oxygen as well as exothermic heat effect were detected in the similar temperature range. This effect is related to the burning of the carbon deposit formed in the previous stages of the thermal transformations of organic matter deposited in the pore system of the PCH samples.

Similar stages of the thermal degradation of template can be distinguished for the as-prepared Ti-containing PCH samples (Figs. 2–4). However, differences in the intensities as well as the positions of the DTG, DTA and ion evolution peaks should be noted. The DTG peak related to desorption of the products of the thermal degradation of templates, which was found for the PCH

sample at 184 °C, is shifted to about 205–208 °C for PCH-1.5Ti and PCH-7.5Ti, while for the sample PCH-15Ti is centered at 239 °C. Additionally, the intensity of this peak gradually decreases with an increase in Ti content. On the other hand, the intensity of DTG peaks attributed to the combustion of organic templates raised when the loading of Ti increases. It should be noted that evolution of trimethylamine occurred at temperature higher by about 40–50 °C for the Ti-containing samples than for PCH. Incorporation of titanium into the PCH structure generated additional acid centers, which probably bonded basic trimethylamine molecules and was the reason why their evolution from these samples was observed at higher temperatures. A similar shift in the evolution temperature of the $m/e = 30$ ions was found. If we assume that these ions are related mainly to the presence of NO, it could be suggested that a part of chemisorbed trimethylamine molecules was oxidized to NO, CO_2 and H_2O in this temperature range.

In contrast to the PCH sample, for the Ti-containing materials, two well-resolved high temperature peaks in DTG curve related to burning of carbon deposit have appeared. Additionally, the evolution of the reaction product- CO_2 , as well as consumption of oxygen occurred in two, well separated stages. Therefore, the presence of two types of carbon deposits, which significantly differs with respect to their reactivity in the oxidation process is suggested.

3.2. Structure, texture and thermal stability of PCH materials

Fig. 5 presents X-ray diffractograms recorded for the sodium form of montmorillonite (Na-Mont) as well as calcined (600 °C) and non-calcined PCHs. For the sodium form of montmorillonite

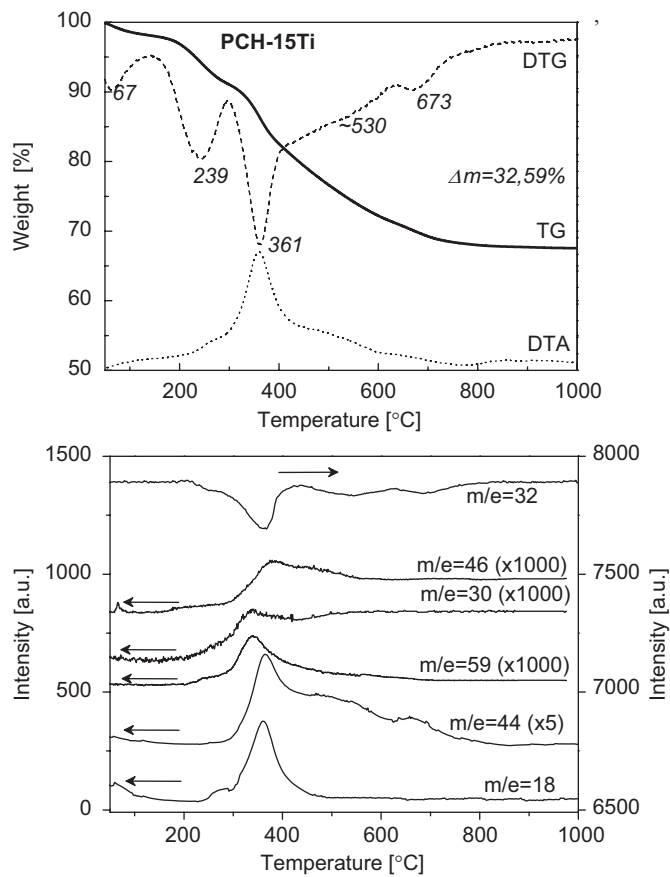


Fig. 4. Results of TG-DTA and evolved gas analysis of the as prepared PCH-15Ti sample.

the diffraction peak d_{001} attributed to the ordering of the clay layers is present in the position (6.83°) related to the basal spacing of 1.26 nm and two dimensional diffractions hk were found at 19.96° and 35.06° [29]. Additionally, the reflection at 2θ of 19.7° corresponding to diffraction from (100) layers of montmorillonite and the reflection at about 27° attributed to the presence of quartz impurities were detected. The basal spacing of the layered clay minerals depends on the thickness of the clay layer and interlayer distance. The thickness of the montmorillonite layers is estimated to be about 0.96 nm [30,31]. Therefore, the interlayer distance is about 0.30 nm, which is typical of hydrated clays [32]. The hk reflections are characteristic for this type of the clay mineral. Each observed hk reflection is the summation of several hk index pairs. The diffraction at 19.96° is the summation of hk indices of (02) and (11), while the diffraction at 35.06° is superposition of (13) and (20) indices [30].

The deposition of surfactants and co-surfactants as well as the formation of the silica or silica-titania pillars in the interlayer space of montmorillonite resulted in a shift of the d_{001} peak in direction of the lower values of 2θ angles. This effect is related to an increase of the interlayer distance in the clay materials. For the PCH sample (non-calcined), the 001 peak was shifted to the position characteristic for the basal spacing of 3.74 nm. Taking into account the thickness of the montmorillonite layer (0.96 nm), it could be calculated that the interlayer distance is about 2.78 nm. Marras et al. [33] showed that the interlayer distance for the HDA molecules oriented perpendicularly in relation to the montmorillonite layers is about 1.44 nm. The value determined in our studies is nearly twice larger, which may suggest the formation of the cylindrical micelles in the interlayer space of the clay. Additionally, the low-intensive peak related to the basal spacing of 0.98 nm was detected. This peak could be attributed to the stacked-together clay layers (not separated by the interlayer space). Such effect is possible when protons or any other small,

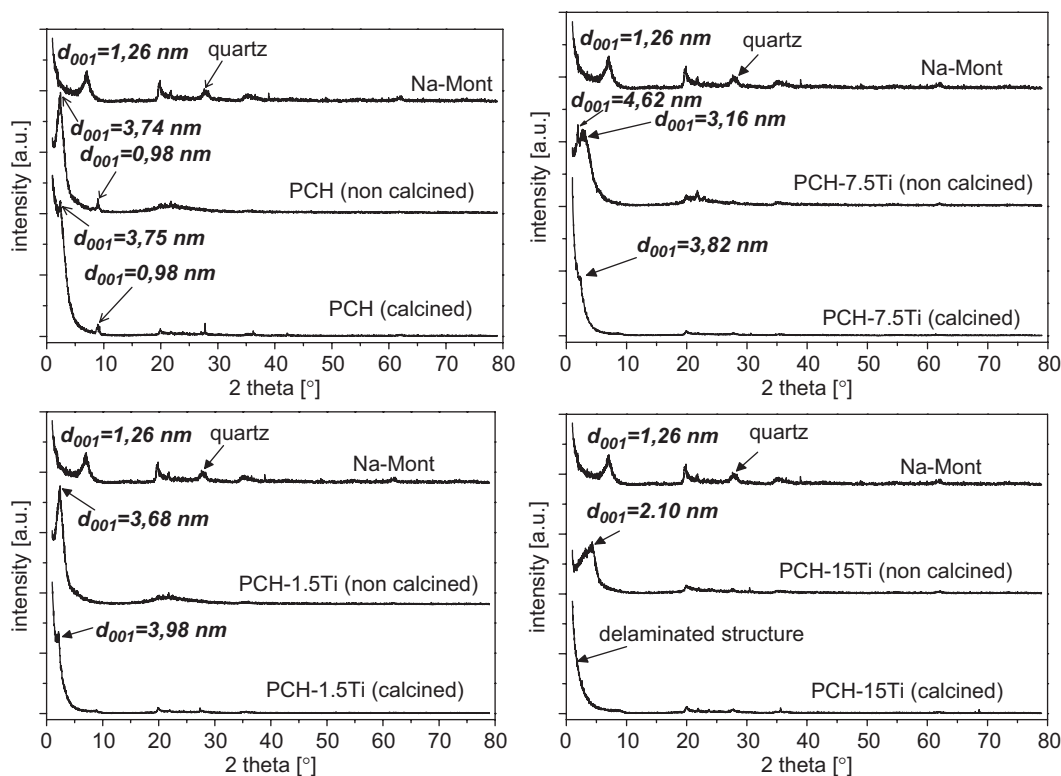


Fig. 5. X-ray diffractograms of the parent clay, as prepared PCHs and calcined PCHs.

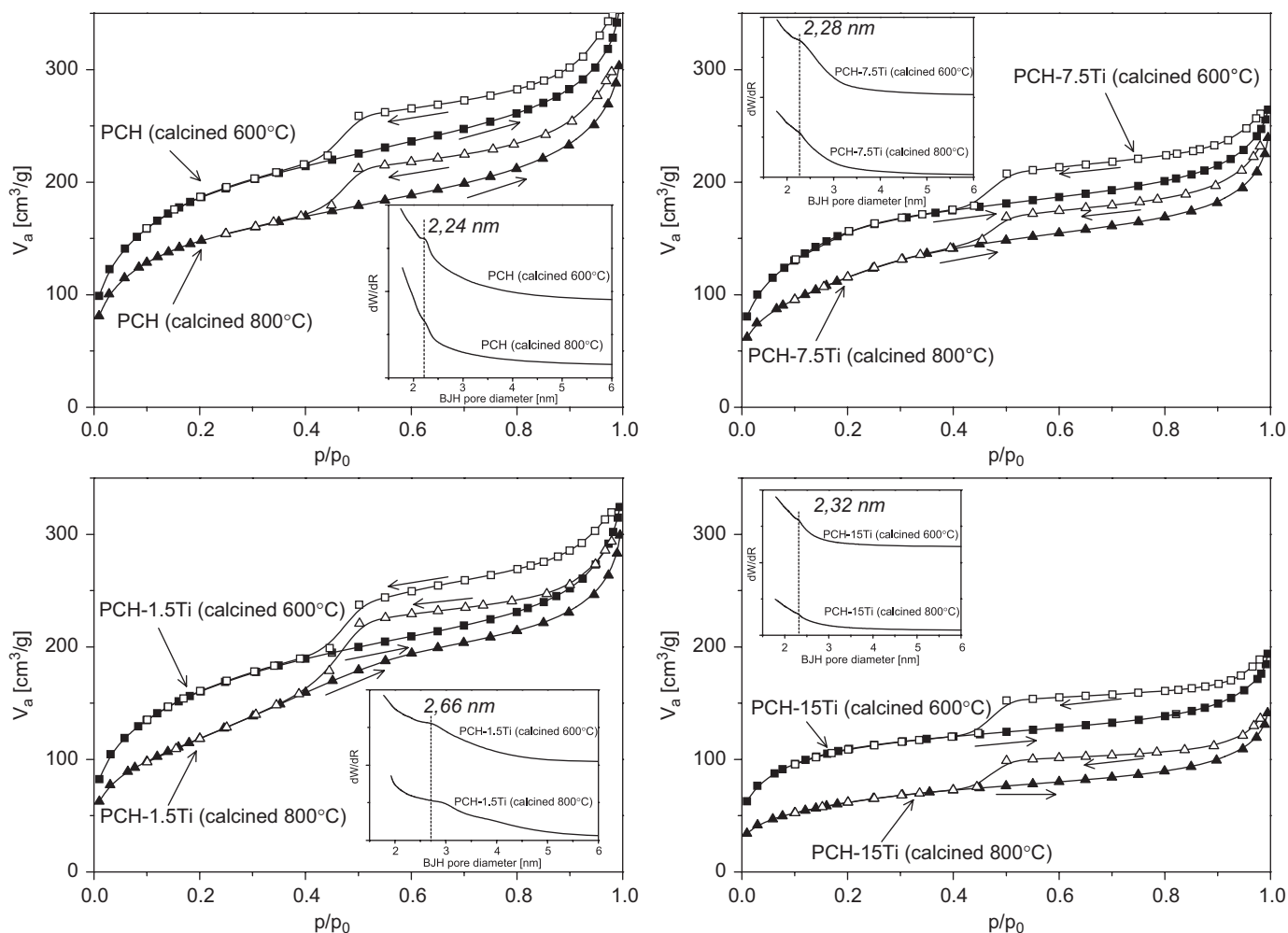


Fig. 6. Adsorption–desorption isotherms and BJH pore size distribution of the PCH samples calcined at 600 and 800 °C.

dehydrated cations migrated from the interlayer space into the clay layers (unoccupied octahedral positions) resulting in the neutralization of the negative charge of the layer [11,34]. Calcination of the sample at temperature 600 °C did not change the positions of the basal peaks, however the intensity of the maximum located in 2θ angle of 2.38° was significantly reduced. Pillared clays that exhibit no 001 reflection have been referred in the literature as “delaminated structure” characterized by not parallel ordering of the clay layers [e.g. 35,36]. Probably the pillared structure of PCHs is stabilized by templates. Oxidation of the templates is an exothermic process and local overheating of the sample may result in disturbing of the layers ordering. Very similar diffractograms were obtained for the sample PCH-1.5Ti. Lack of the peak related to the presence of the stacked clay layers and small disparity in the position of basal peaks are the only found differences.

For the samples containing larger amount of titanium (PCH-7.5Ti and PCH-15Ti), the intercalation of surfactant and co-surfactant molecules as well as precursors of the inorganic pillars (TEOS, TIP) into the interlayer space also resulted in an expanding of the basal spacing of the clay. This effect is manifested by a shift of the 001 peak in a direction of lower values of 2θ angles. However, in this case the basal peaks recorded for the non-calcined samples are much broader and are in the positions different than these found for the PCH and PCH-1.5Ti samples. For the PCH-7.5Ti a broad maximum centered at about 2.78° ($d_{001} = 3.16$ nm) and sharp peak at 1.92° ($d_{001} = 4.62$ nm) were

found. If we take into account that the thickness of the montmorillonite layer is 0.96 nm, the interlayer distance related to these peaks is 2.20 and 3.66 nm, respectively. For PCH-15Ti (non-calcined sample) the very broad 001 peak at about 4.21° ($d_{001} = 2.10$ nm) was found. The obtained results suggest that for the samples containing higher loading with titania the surfactant and co-surfactant molecules apart from cylindrical micelles form other type of aggregates. Marras et al. [33] proposed the various orientations of HDA molecules in the interlayer space of montmorillonite and related to them basal spacings. Calcination of the PCH-7.5Ti and PCH-15Ti samples resulted in a disappearance of the 001 reflection. Therefore, it seems that also in this case the calcined samples are characterized by the delaminated structure.

The nitrogen sorption–desorption isotherms as well as BJH pore size distributions (calculated from the adsorption branches of isotherms) for PCHs calcined at 600 and 800 °C are presented in Fig. 6. A gradual increase in nitrogen sorption observed at low to medium partial pressure ($p/p_0 < 0.3$) suggests the presence of supermicropores and small mesopores [23]. An increase in adsorbed volume observed at higher partial pressures could be related to larger mesopores. This effect is more pronounced for the PCH and PCH-1.5Ti samples than for the PCH materials containing the larger concentration of titanium (PCH-7.5Ti and PCH-15Ti). The hysteresis loops could be qualified to the H4 type, corresponding to the aggregates forming the slit-like pores with uniform sizes [37]. The BET surface areas (S_{BET}) and pore volumes

Table 1
Textural parameters of PCHs calcined at various temperatures.

Sample	Calcination temperature (°C)					
	550		600		800	
	S_{BET} (m ² /g)	V_{p} (cm ³ /g)	S_{BET} (m ² /g)	V_{p} (cm ³ /g)	S_{BET} (m ² /g)	V_{p} (cm ³ /g)
PCH	579	0.47	675	0.49	531	0.42
PCH-1.5Ti	477	0.44	587	0.45	436	0.41
PCH-7.5Ti	501	0.37	573	0.37	425	0.32
PCH-15Ti	367	0.35	390	0.27	225	0.19

Table 2
Chemical composition of sodium form of montmorillonite and the PCH samples calcined at 600 °C.

Sample	Na ₂ O	K ₂ O	MgO	CaO	Al ₂ O ₃	SiO ₂	Fe ₂ O ₃	TiO ₂
Mt-Na	2.37	1.03	1.60	0.80	21.91	69.15	3.03	0.11
PCH	0.28	0.12	0.80	0.00	9.98	87.44	1.49	0.05
PCH-1.5Ti	0.14	0.13	0.71	0.00	12.59	82.06	1.99	2.37
PCH-7.5Ti	0.51	0.05	1.07	0.08	14.89	76.89	1.82	4.68
PCH-15Ti	0.39	0.00	1.13	0.00	16.19	71.55	2.30	8.43

(V_{p}) of PCHs calcined at temperatures 550, 600 and 800 °C are compared in Table 1. Regardless the calcination temperature, the highest values of these parameters were found for the PCH sample. Introduction of titanium into the PCH structure resulted in a gradual decrease in S_{BET} and V_{p} . Calcination of as-prepared PCHs at 600 °C produced materials characterized by significantly higher surface areas comparing to the samples calcined at lower (550 °C) or higher (800 °C) temperatures. This effect could be attributed to an incomplete removal of the carbon deposits (formed during thermal decomposition of organic templates) at 550 °C. On the other hand, a partial collapse of the porous structure could occur at temperature as high as 800 °C. It should be noted that such drastic calcination conditions (800 °C/6 h) reduced the surface areas and pore volumes by 21.3–42.3% and 8.9–29.6%, respectively.

The chemical composition of montmorillonite (sodium form) and the PCH samples (calcined at 600 °C) is presented in Table 2. The layer of montmorillonite consists of the octahedral alumina sublayer, which is located between two tetrahedral silica sheets. A part of Al³⁺ cations located in the octahedral sublayer of the clay is substituted by Mg²⁺ ions, while Na⁺, K⁺, Ca²⁺ and possibly also Mg²⁺ cations are located in the interlayer space of montmorillonite and compensate the negative charge of the clay layers. Iron and titanium are typical impurities of natural clay minerals, however iron can also occupy octahedral positions in the montmorillonite layers. It should be noted that the content of interlayer cations in the parent clays was significantly higher than in the PCH materials. This effect is related to the exchange of these cations by the HDTMA ions, which is the first step of the PCH synthesis. The deposition of the silica or silica–titania pillars into the interlayer space of the clays significantly increased the content of SiO₂ and TiO₂ in the PCH materials.

The coordination of transition metals present in the samples was studied by UV–vis–DR spectroscopy. Fig. 7 presents the spectrum recorded for the PCH sample calcined at temperature of 600 °C. This spectrum consists of the broad adsorption peak detected in the range of 200–450 nm. The PCH sample contained significant amount of iron (Table 2), which is a natural component of montmorillonite. Presented in literature UV–vis–DR spectra of the iron containing samples are characterized by the bands

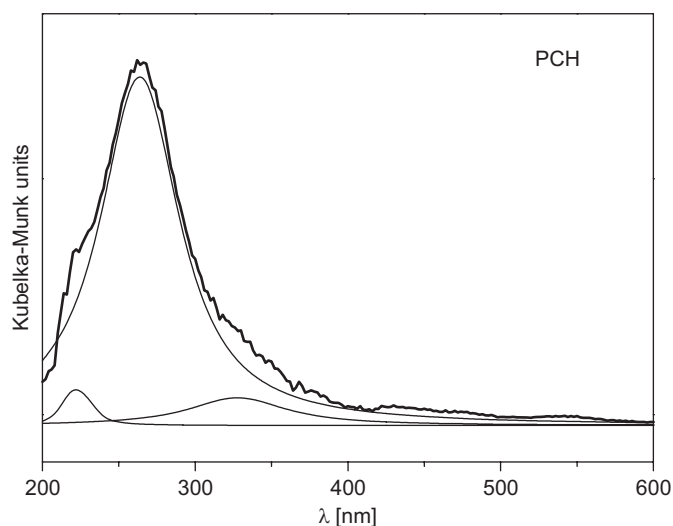


Fig. 7. UV–vis–DR spectrum recorded for the PCH sample.

related to Fe³⁺ ← O charge transfer. The position of these bands depends on the coordination and agglomeration of iron (III) species [38,39]. Mononuclear Fe³⁺ cations give rise to the bands in the range of 200–300 nm. The bands in the region of 300–400 nm are characteristic of small oligonuclear Fe_xO_y clusters, while bulky particles of Fe₂O₃ give characteristic bands above 400 nm [40]. Additionally, in the case of isolated Fe³⁺ cations a distinction between iron ions in the tetrahedral (band below 250 nm) and octahedral (band in the range of 250–300 nm) coordination is possible [38,39]. The spectrum recorded for the PCH sample was deconvoluted into three sub-bands. The most intensive sub-band centered in the range of 250–300 nm is related to the isolated Fe³⁺ cations located in the octahedral positions of the clay layers. Only minute band was found for mononuclear iron (III) ions in the tetrahedral coordination as well as for small oligonuclear Fe_xO_y clusters. Therefore, it could be concluded that Fe³⁺ cations are located nearly exclusively in the octahedral positions of the clay layers. Small amounts of iron are present in the tetrahedral

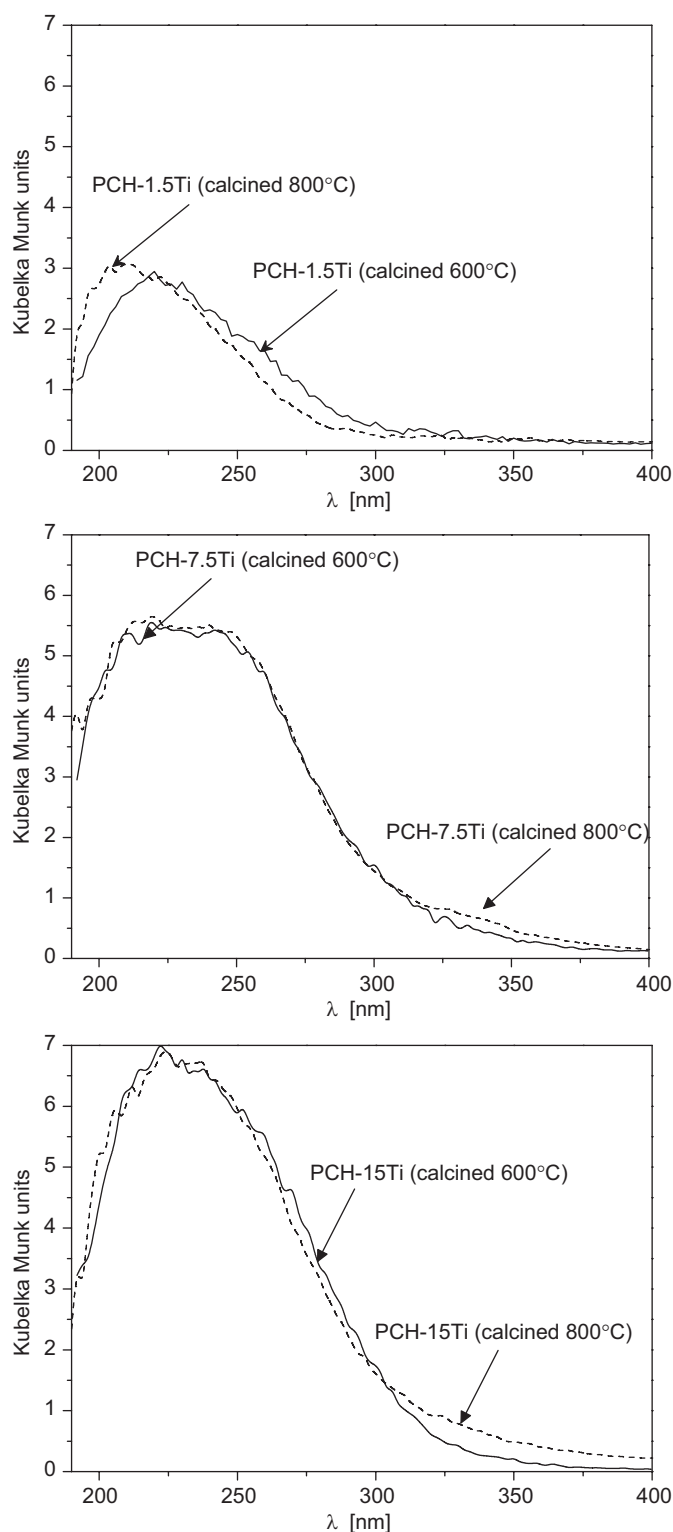


Fig. 8. Differential UV-vis-DR spectra recorded for the Ti-modified samples calcined at 600 and 800 °C.

sublayers and in the form of small iron oxide clusters in the interlayer space of the clay or surface of clay particles. Apart from iron, the PCH sample contains also small contribution of titanium, which is characterized by adsorption peaks in the range similar to those typical of iron species [41]. However, it should be noted that the molar ratio Fe/Ti in the PCH sample is higher than 30 and

therefore, the contribution of titanium species to the spectrum is negligible.

The UV-vis-DR spectra recorded for the Ti-containing samples are presented in Fig. 8. It should be mentioned that these spectra are the results of the subtraction of the original spectra recorded for the PCH sample from the original spectra of the titanium containing sample. Therefore, the spectra presented in Fig. 8 are related only to the titanium present in the PCH samples calcined at temperature of 600 and 800 °C. For the samples containing titanium, some bands characteristic of this metal in different coordination and aggregation have been proposed. The bands at about 205–220 nm are related to the presence of Ti^{4+} ions in the tetrahedral coordination (i.e. titanium incorporation into the framework of the silica matrix), which are assigned to a charge transition in $[\text{TiO}_4]$ and $[\text{O}_3\text{Ti}-\text{OH}]$ moieties [41–43]. Isolated extraframework Ti^{4+} cations in the octahedral coordination would give a charge transfer at about 230 nm. Partially polymerized hexacoordinated titanium species, which contain Ti–O–Ti bridges and belong to a silicon-rich amorphous phase, would exhibit a band at about 270 nm [44]. Anatase clusters are characterized by the band situated at about 330 nm [41].

For the sample PCH-1.5Ti calcined at 600 °C a broad maximum centered at about 220 nm was found. Therefore, it could be supposed that the majority of Ti ions was incorporated into silica matrix in the form of tetraordinated titanium. An increase in the calcination temperature to 800 °C resulted in a shift of the maximum of the band to about 208 nm. This effect could be related to the incorporation of the part of the isolated extraframework hexacoordinated Ti^{4+} ions (possibly coordinated by H_2O [45]) into the silica framework in the form of isolated tetraordinated cations. It should be noted that there are not bands characteristic for the presence of anatase neither for the sample calcined at 600 nor 800 °C. The bands found for the samples with higher concentration of titanium (PCH-7.5Ti and PCH-15Ti) are shifted in direction of higher values of wavelength comparing to the PCH-1.5Ti sample. This effect is probably related to the significant contribution of titanium in the form of polymerized species. An increase in the calcination temperature from 600 to 800 °C slightly increased the intensity of light adsorption in the range of 310–420 nm, suggesting formation of anatase clusters. The peaks characteristic for anatase were not detected in the XRD measurements, therefore the size of its crystals is probably below the detection level of this method.

3.3. Surface acidity of PCH materials

The surface acidity of the PCHs was studied by two methods. The surface concentration of acid sites and their strength was determined by temperature programmed desorption of ammonia (NH_3 -TPD), while FT-IR analysis of the samples with adsorbed pyridine was used for the evaluation of the contribution of the Brønsted and Lewis acid centers.

Fig. 9 presents the results NH_3 -TPD measurements (desorption curves), while in Table 3 the data related to the surface concentration of chemisorbed ammonia are summarized. Desorption of ammonia proceeded in the relatively broad temperature range of 100–500 °C. The surface concentration of chemisorbed ammonia increased with rising in titanium content. Therefore, it could be concluded that titanium introduced into the PCH structure generated acid sites. For the samples PCH, PCH-7.5Ti and PCH-15Ti the maximum of the ammonia desorption was found at about 200–220 °C. Desorption of ammonia from the PCH-1.5Ti proceeds in two steps represented by peaks centered at 170 and 270 °C. It should be noted that chemisorbed ammonia covers the fraction of the sample surface lower than 7.5% (assuming formation of monolayer).

The type of acid sites present in the PCH samples was tested by pyridine adsorption, followed by IR spectroscopy. Pyridine was adsorbed at 170 °C in all the clays (activated at 550 °C) and subsequently desorbed at the adsorption temperature for 20 min to remove weakly bonded pyridine molecules. The selected spectra, for PCH and PCH-15Ti are presented in Fig. 10A and B, respectively.

All the Ti-containing PCH samples exhibited similar amount of Brønsted (band at 1540 cm⁻¹) and Lewis (band at 1450 cm⁻¹) acid sites. The number of Brønsted centers increased twice, comparing to pure PCH sample, while the number of Lewis sites stayed at the

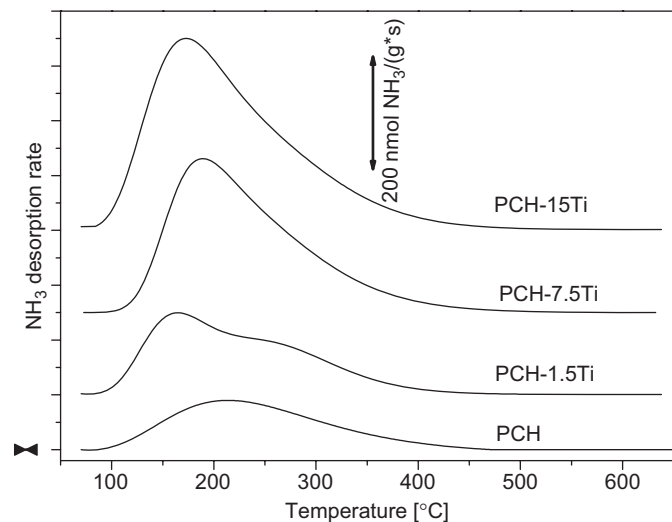


Fig. 9. Results of NH₃-TPD measurements performed for a series of the PCH samples.

Table 3

Comparison of ammonia chemisorption on the surface PCHs calcined at 600 °C.

Sample	NH ₃ sorption (μmol NH ₃ /g)	Surface concentration of chemisorbed NH ₃ (μmol/m ²)	Coverage of surface by NH ₃ ^a (%)
PCH	97.1	0.144	1.30
PCH-1.5Ti	147.3	0.251	2.27
PCH-7.5Ti	238.2	0.416	3.75
PCH-15Ti	320.6	0.822	7.43

^a Percentage of the surface covered by a monolayer of chemisorbed ammonia. It was assumed that the surface occupied by one NH₃ molecule is 0.15 nm² [46].

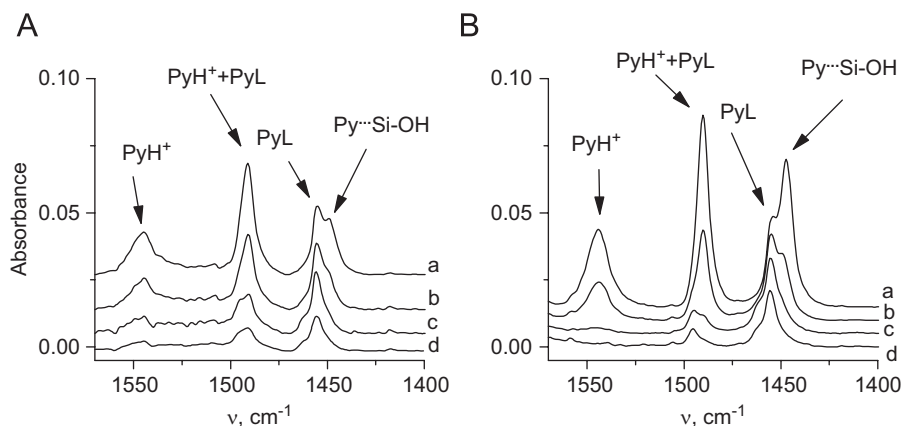


Fig. 10. IR spectra of pyridine adsorbed on PCH (A) and PCH-15Ti (B). Spectra recorded after 20 min pyridine desorption at 170 °C (a), 250 °C (b), 350 °C (c) and 450 °C (d). All spectra recorded at 170 °C, normalized to the mass of the “standard” 10 mg pellet.

same level, independently of the amount of introduced titanium. This means that titanium was not introduced in the form of bulky oxides, which should play the role of the Lewis acids [47]. It should be noted that the formation of bulky titania clusters was also not detected by UV–vis-DRS analysis of the Ti-modified samples. What is more, the Lewis acidity is the intrinsic feature and is independent of the post-synthesis modification of the sample.

Specific feature of this series of PCH is the enhanced acidity of their silanol groups. After desorption at 170 °C quite intensive band at 1448 cm⁻¹ appeared on the spectrum. This band is characteristic of pyridine hydrogen-bonded to silanol Si–OH groups (Fig. 10A and B, spectra a). At the same time, the red-shift of the band of silanol group was observed (spectra not shown). What is interesting, hydrogen-bonded pyridine is still present for all the Ti-containing clays and pure PCH at desorption temperature as high as 250 °C (Fig. 10A and B, spectra b). It is known that in microporous structures, such as zeolites, the presence of a strong Lewis site can significantly enhance the acidity of the nearby Brønsted center [47,48].

The amount of Brønsted sites (OH groups other than silanols) was calculated from the intensity of the 1540 cm⁻¹ PyH⁺ pyridinium ions band and its absorption coefficient equal 0.078 cm/μmol, as determined in our previous work [49]. At the same time, the number of coordinated pyridine molecules (pyridine bonded onto Lewis sites, PyL) can be determined from the intensity of the 1450 cm⁻¹ band and its absorption coefficient equal 0.165 cm/μmol, as determined in our previous work [50]. The results were summarized in Table 4. An increase in the contributions of Brønsted centers can be explained by the presence of titanium cations of higher than four-fold coordination. It was already proposed by Tanabe et al. [51] that Ti cations of coordination number four are the source of the Lewis acidity, while those of coordination number six, can be a source of the

Table 4
Contribution of Brønsted (B) and Lewis (L) acid centers (%) and A_{des}/A_{170} values for PCHs.

Sample	Desorption temperature (°C)	Contribution of sites (%)		A_{des}/A_{170}	
		B	L	B	L
PCH	170	34.0	66.0	1.00	1.00
	250	28.9	71.1	0.62	0.78
	350	18.0	82.8	0.31	0.72
	450	0.0	100.0	0.00	0.58
PCH-1.5Ti	170	43.9	56.1	1.00	1.00
	250	30.5	69.5	0.52	0.93
	350	16.9	83.1	0.22	0.83
	450	0.0	100.0	0.00	0.67
PCH-7.5Ti	170	53.9	46.1	1.00	1.00
	250	47.7	52.3	0.56	0.91
	350	14.4	85.6	0.11	0.77
	450	0.0	100.0	0.00	0.41
PCH-15Ti	170	56.4	43.6	1.00	1.00
	250	40.0	60.0	0.48	0.94
	350	0.0	100.0	0.00	0.84
	450	0.0	100.0	0.00	0.63

Brønsted acidity. For the latter case the excess of the negative charge of -2 is distributed on six Ti–O bonds and should generate Brønsted acidity.

The relative acid strength of both Brønsted and Lewis sites was estimated in thermodesorption experiments, in which pyridine was stepwise desorbed at increasing temperatures (170, 250, 350 and 450 °C) and after each desorption step the spectrum was recorded at 170 °C (Fig. 10A and B). The value A_{des}/A_{170} is a measure of the strength of the acid sites. In this fraction, A_{170} is the intensity of PyH⁺ or PyL bands after pyridine desorption at 170 °C and A_{des} is the intensity of PyH⁺ or PyL bands after pyridine desorption at higher temperature (250, 350, 450 °C). The higher is the value of A_{170}/A_{des} , the higher is the strength of particular acid centers. From presented fractions A_{170}/A_{350} should be used (desorption at 350 °C), as 250 °C was not enough to desorb pyridine from silanol groups, thus is too low to discriminate stronger and weaker sites, and 450 °C is too high as it is able to almost completely remove pyridine from the clays. In this series, PCH-1.5Ti contained the strongest Brønsted sites, and PCH-15Ti—the weakest. Therefore, an incorporation of the small amount of titanium caused an increase in the acid strength of Brønsted sites, but when more Ti atoms were introduced, the strength was again lowered. On the other hand, the strength of the Lewis sites stayed at the same level for all the samples, independently of the titanium loading, once again suggesting that introduced titanium is not a source of the Lewis-type acidity.

4. Conclusions

The montmorillonite-based PCH materials intercalated with silica–titania pillars was synthesized and characterized. Thermal degradation of surfactant and co-surfactant molecules present in the pore system of the as-prepared PCH samples proceeded in few stages. At relatively low temperatures evolution of products of the surfactant and co-surfactant fragmentation occurred. Intensive evolution of CO₂ and H₂O observed at higher temperatures suggested that the oxidation of the organic matter present in PCHs was the next step of surfactant and co-surfactants removal.

Part of organic matter was transformed into thermally stable carbon deposits, which were oxidised at temperatures above 450–500 °C. Calcination of the as-prepared PCH samples at temperature 550 °C did not guarantee complete removal of the organic species from the pore system of the samples, while calcination at temperature 800 °C resulted in a partial collapse of the pillared structure of PCHs.

PCHs were characterized with respect to their textural parameters, chemical nature of titanium incorporated into the PCH structure as well as surface acidity. For the samples with the low titanium loading, the isolated Ti⁴⁺ cations in the tetrahedral coordination dominated. An increase in titanium content as well as calcination temperature resulted in the formation of the polymeric metal oxide species and also small amount of anatase clusters. An incorporation of titanium into the silica pillars significantly increased surface acidity of the PCH samples mainly by generation of the Brønsted-type acidity. The surface area and porosity of the PCHs decreased with the increase of titanium content.

Acknowledgments

Authors acknowledge the Polish Ministry of Science for financial support in the frame of project N597 150 32/4091 and S&B Industrial Minerals GmbH for supplying of montmorillonite.

References

- [1] W.D. Jones, *Ann. Rev. Earth Planet* 7 (1979) 183.
- [2] R.W. Hoffmann, G.W. Brindley, *Am. Mineral.* 46 (1961) 450.
- [3] R.T. Yang, N. Tharappiwattananon, R.Q. Long, *Appl. Catal. B* 19 (1998) 289.
- [4] M.A. Vicente, M.A. Banares-Munoz, L.M. Gandia, A. Gil, *Appl. Catal. A* 217 (2001) 191.
- [5] R.Q. Long, R.T. Yang, *Appl. Catal. B* 24 (2000) 13.
- [6] L. Chmielarz, P. Kuśtrowski, M. Zbroja, A. Rafalska-Lasocha, D. Dudek, R. Dziembaj, *Appl. Catal. B* 45 (2003) 103.
- [7] P.X. Wu, A.W. Liao, H.F. Zhang, J.C. Guo, *Environ. Int.* 26 (2001) 401.
- [8] H.J. Chae, I.S. Nam, S.W. Ham, S.B. Hong, *Catal. Today* 68 (2001) 31.
- [9] F. González, C. Pesquera, I. Benito, E. Herrero, C. Poncio, S. Casuscelli, *Appl. Catal. A* 181 (1999) 71.
- [10] H.Y. Zhu, E.F. Vansant, J.A. Xia, G.Q. Lu, *J. Por. Mater.* 4 (1997) 17.
- [11] A. Galarneau, A. Barodawalla, T.J. Pinnavaia, *Nature* 374 (1995) 529.
- [12] L. Chmielarz, P. Kuśtrowski, R. Dziembaj, P. Cool, E.F. Vansant, *Catal. Today* 114 (2006) 319.
- [13] L. Wei, T. Tang, B. Huang, *Micropor. Mesopor. Mater.* 67 (2004) 175.
- [14] J. Ahenach, P. Cool, E.F. Vansant, *Phys. Chem. Chem. Phys.* 2 (2000) 5750.
- [15] O.Y. Kwon, H.S. Shin, *Chem. Mater.* 12 (2000) 1273.
- [16] L. Chmielarz, P. Kuśtrowski, Z. Piwowarska, B. Dudek, B. Gil, M. Michalik, *Appl. Catal. B*, doi: 10.1016/j.apcatb.2008.11.001.
- [17] K. Schrijnemakers, N.R.E.N. Impens, E.F. Vansant, *Langmuir* 15 (1999) 5807.
- [18] Z. Ding, Y. Zhu, P.F. Greenfield, G.Q. Lu, *J. Colloid Interface Sci.* 238 (2001) 267.
- [19] C.H. Zhou, Z.H. Ge, X.N. Li, H.Q. Guo, J. Sun, *Chin. Chem. Lett.* 14 (2003) 1285.
- [20] Z. Liu, J. Tabora, R.J. Davis, *J. Catal.* 149 (1994) 117.
- [21] M. Polverejan, Y. Liu, T.J. Pinnavaia, *Chem. Mater.* 14 (2002) 2283.
- [22] C. Zhou, X. Li, Z. Ge, Q. Li, D. Tong, *Catal. Today* 93–95 (2004) 607.
- [23] M. Benjelloun, P. Cool, T. Linssen, E.F. Vansant, *Micropor. Mesopor. Mater.* 49 (2001) 83.
- [24] M. Benjelloun, P. Cool, T. Linssen, E.F. Vansant, *Phys. Chem. Chem. Phys.* 4 (2002) 2818.
- [25] J. Ryczkowski, J. Gaworek, W. Gac, S. Pasieczna, T. Borowiecki, *Thermochem. Acta* 434 (2005) 2.
- [26] J. Park, S.C. Jana, *Polymer* 45 (2004) 7673.
- [27] J. Gaworek, W. Stefania, A. Kierys, M. Iwan, J. Therm. Anal. Calorim. 87 (2007) 217.
- [28] J. Ravichandran, C.M. Lakshmanan, B. Sivasankar, *React. Kinet. Catal. Lett.* 59 (1996) 301.
- [29] J.P. Chen, M.C. Hausladen, R.T. Yang, *J. Catal.* 151 (1995) 135.
- [30] G.W. Brindley, R.W. Hoffmann, *Clays Clay Miner.* 9 (1962) 546.
- [31] S. Xu, S.A. Boyd, *Langmuir* 11 (1995) 2508.
- [32] M. Kawano, M. Tomita, *Clays Clay Miner.* 39 (1991) 174.
- [33] S.I. Marres, A. Tsimpliaraki, I. Zuburtikudis, C. Panayiotou, *J. Colloid Interface Sci.* 315 (2007) 520.
- [34] L. Chmielarz, P. Kuśtrowski, M. Drozdek, R. Dziembaj, P. Cool, E.F. Vansant, *Catal. Today* 119 (2007) 181.
- [35] R. Burch, *Catal. Today* 2 (1988) 185.

- [36] T.J. Pinnavaia, M.S. Tzou, S.D. Landau, R. Raythatha, J. Mol. Catal. 27 (1984) 195.
- [37] S.J. Greek, K.S.W. Sing, Adsorption, Surface Area and Porosity, Academic Press, London, 1982.
- [38] J. Pérez-Ramírez, M.S. Kumar, A. Brückner, J. Catal. 223 (2004) 13.
- [39] M.S. Kumar, M. Schwidder, W. Grünert, A. Brückner, J. Catal. 227 (2004) 384.
- [40] M.S. Kumar, J. Pérez-Ramírez, M.N. Debbagh, S. Smarsly, U. Bentrup, A. Brückner, Appl. Catal. B 62 (2006) 244.
- [41] Y. Segura, L. Chmielarz, P. Kuśtrowski, P. Cool, R. Dziembaj, E.F. Vansant, Appl. Catal. B 61 (2005) 69.
- [42] A. Corma, Chem. Rev. 97 (1997) 2373.
- [43] T. Blanco, A. Corma, M.T. Navarro, J. Pérez-Parianta, J. Catal. 156 (1995) 65.
- [44] X.F. Li, H.X. Gao, G.J. Jin, L. Chen, L. Ding, H.Y. Yang, Q.L. Chen, J. Mol. Struct. 872 (2008) 10.
- [45] C. Jin, G. Li, X. Wang, Y. Wang, L. Zhao, D. Sun, Micropor. Mesopor. Mater. 111 (2008) 236.
- [46] A.L. McClellan, H.F. Harnsberger, J. Colloid Interface Sci. 23 (1966) 577.
- [47] G.A. Eimer, S.G. Casascelli, C.M. Chanquia, V. Elias, M.E. Crivello, E.R. Herrero, Catal. Today 133–135 (2008) 639.
- [48] E. Brunner, H. Ernst, D. Freude, M. Hunger, C.B. Krause, D. Prager, W. Reschetilowski, W. Schwieger, K.H. Bergk, Zeolites 9 (1989) 282.
- [49] J. Datka, B. Gil, A. Kubacka, Zeolites 18 (1997) 245.
- [50] J. Datka, B. Gil, A. Kubacka, Zeolites 17 (1996) 428.
- [51] K. Tanabe, T. Sumiyoshi, K. Shibata, T. Kiyoura, J. Kitagawa, Bull. Chem. Soc. Jpn. 47 (1974) 1064.